2-1-1998

Derivation of an Analytical Model to Calculate Junction Depth in HgCdTe Photodiodes

Stacy H. Gleixner
San Jose State University, stacy.gleixner@sjsu.edu

H. G. Robinson
SRI International

C. R. Helms
Stanford University

Derivation of an analytical model to calculate junction depth in HgCdTe photodiodes

S. Holander-Gleixner[a)]
Department of Materials Science and Engineering, Stanford University, Stanford, California 94305

H. G. Robinson and C. R. Helms
Department of Electrical Engineering, Stanford University, Stanford, California 94305

(Received 23 May 1997; accepted for publication 20 October 1997)

An enhanced analytical model is derived to calculate the junction depth and Hg interstitial profile during n-on-p junction formation in vacancy-doped HgCdTe. The enhanced model expands on a simpler model by accounting for the Hg interstitials in the p-type, vacancy-rich region. The model calculates junction depth during both the initial, reaction-limited regime of junction formation and the diffusion-limited regime. It also calculates junction depth under conditions when the abrupt junction approximation of the simpler model fails. The enhanced model can be used to determine the limits of the annealing conditions and times for which the junction depth calculated analytically is valid. The decay length of interstitials into the p-type region estimated analytically places an upper bound on the grid spacing needed to accurately resolve the junction in a numerical simulation.
 [S0021-8979(98)03403-3]

I. INTRODUCTION

HgCdTe is a variable band-gap semiconductor used for mid- and long-wavelength, infrared detectors. Because the Te-rich side of HgCdTe's existence region is large, the Hg vacancy concentration in Te-rich HgCdTe can be quite high ($>1\times10^{16}$ cm^{-3}). Te-rich HgCdTe is p type due to the doubly negative charge of these Hg vacancies.[1] N-on-p photodiodes are formed in Te-rich HgCdTe by injecting Hg interstitials, which annihilate Hg vacancies, revealing a lower concentration, background donor. The electrical junction exists at the boundary between high and low vacancy concentrations. Excess Hg interstitials can be injected through several different processes including annealing in a Hg-rich ambient, ion implantation, and ion milling.[2–9]

The junction depth as a function of time is determined by the nature of the Hg interstitial source, the Hg interstitial diffusion coefficient, the background Hg vacancy concentration, and the annealing temperature. When excess Hg interstitials diffuse into HgCdTe, there is an initial reaction-limited regime where interstitials recombine with vacancies at the surface. The Hg interstitial concentration decays exponentially into the HgCdTe due to a finite recombination rate with the vacancies. The junction drive-in rate is linear with time. After a short time, the Hg interstitial and vacancy concentrations at the surface equilibrate at the Hg-rich phase limit. Excess interstitials must then diffuse through the Hg-rich region to the vacancy-rich bulk to reach the recombination sites. Junction drive-in becomes limited by the diffusion of the interstitials through the Hg-rich region. The resistance of the material to further junction drive-in increases as the width of the n-type region increases; the drive-in rate is proportional to the square root of time. This regime is known as the parabolic regime.

A previously developed numerical model has proven to be very successful at simulating n-on-p junction formation.[10–14] This model is based on the simultaneous solution of coupled partial differential equations for the dominant point defects. In this paper, we compare the numerical model to an analytical solution of the junction formation process. The analytical model is similar to the linear–parabolic model developed by Deal and Grove for the oxidation of silicon.[15] An enhanced version of the analytical model has been derived to account for the Hg interstitials in the p-type region. The analytical model employs fewer parameters than the numerical model, making it easier to determine the influence of each parameter on junction depth and shape. By accounting for the decay of interstitials into the p-type region, the enhanced model makes it possible to calculate junction depth during the initial, reaction-limited regime of junction formation, as well as during the diffusion-limited regime. The enhanced model can also be used to determine the limits of when an analytical solution is valid. The exponential decay of interstitials calculated in the enhanced model can be used to determine an upper bound on the grid spacing used in numerical simulations. The grid spacing should be less than the decay length in order to accurately resolve the junction.

II. OVERVIEW OF THE NUMERICAL MODEL

Junction formation in intrinsically doped HgCdTe occurs when excess Hg interstitials (Hg_I) recombine with Hg vacancies (V_{Hg}), revealing a grown-in, background donor. The generation and recombination of Hg vacancies and interstitials are controlled by

$$Hg_{Hg} \underset{k_R}{\overset{g}{\rightleftarrows}} V_{Hg} + Hg_I, \tag{1}$$

where g and k_R are the rates at which the point defects are generated and recombine, respectively.

The junction depth and shape are determined not only by the rates at which the point defects interact but also by dif-

a)Electronic mail: stacy@leland.stanford.edu

fusion of the point defects. The continuity equations for Hg interstitials and vacancies due to the combination of diffusion and generation/recombination are

$$\frac{\partial C_I}{\partial t} = D_I \frac{\partial^2 C_I}{\partial x^2} + g - k_R C_I C_V, \tag{2}$$

and

$$\frac{\partial C_V}{\partial t} = D_V \frac{\partial^2 C_V}{\partial x^2} + g - k_R C_I C_V, \tag{3}$$

where C_I and C_V are the concentrations of Hg interstitials and vacancies, and D_I and D_V are their respective diffusion coefficients. These coupled differential equations are the same as those used to model point defect interactions in Si and GaAs.[16–18] They can be solved numerically to give point defect profiles as a function of depth, time, initial conditions, and processing conditions.[10–14,16–18] Using a simple boundary condition of the surface as a recombination site for point defects, the simulation requires eight (seven independent) parameters.[12] These are D_I, D_V, C_I^{equil}, C_V^{equil}, g, k_R, and the surface recombination velocities (k_I^{surf} and k_V^{surf}). More parameters are needed for complex boundary conditions such as segregation or injection of the point defects at the surface.[19] Several of these parameters have been determined from Hg self-diffusion experiments and from electrical measurements of the vacancy concentration.[12,13] The numerical model accurately simulates data over a range of initial conditions and processing conditions including junction formation by annealing in a Hg ambient[12,13] and junction formation by ion implantation.[19]

III. DERIVATION OF A SIMPLIFIED ANALYTIC MODEL

Under certain conditions, simpler analytical methods can be used to quickly calculate critical information such as junction depth as a function of annealing time, annealing temperature, and initial vacancy concentration. The use of an analytical model reduces the number of parameters involved and provides enhanced insight into the mechanisms underlying Eqs. (1)–(3). In the analytical model, the material is divided into two regions, as seen in Fig. 1(a). In region I, the interstitials are assumed to be in steady state. In addition, equilibrium between the interstitials and vacancies is also assumed ($g = k_R C_I C_V$). This reduces Eq. (2) to

$$\frac{\partial C_I}{\partial t} = D_I \frac{\partial^2 C_I}{\partial x^2} = 0. \tag{4}$$

In the simple analytical model, a further assumption is made that the interstitial concentration at the interface between regions I and II is zero. This leads to

$$C_I = C_I^{\text{surface}} \left(\frac{x_j - x}{x_j} \right), \tag{5}$$

where C_I^{surface} is the steady state, Hg interstitial concentration at the surface, and x_j is the junction depth, the depth of the interface between regions I and II. An infinite source of Hg interstitials is assumed in order to maintain C_I^{surface} over time.

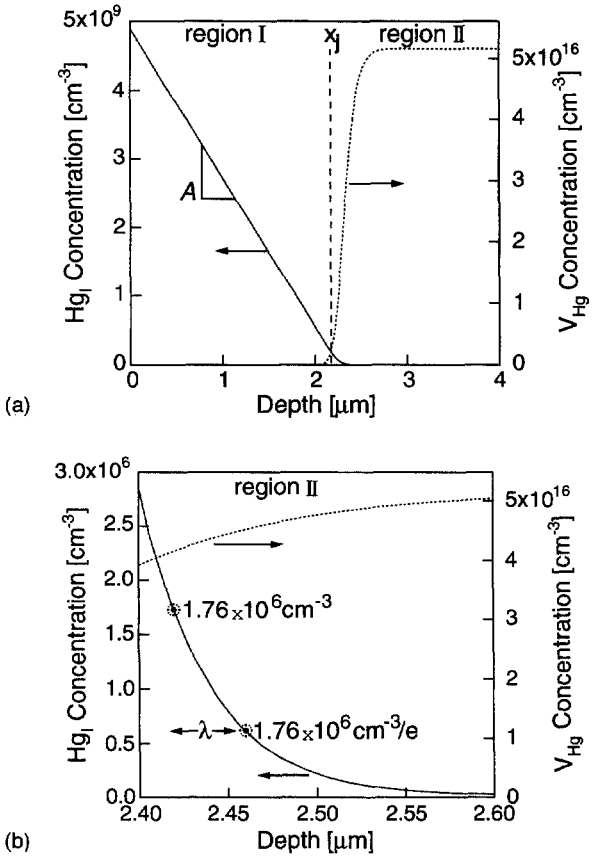

FIG. 1. (a) Hg interstitial and vacancy profiles resulting from a numerical solution of a 2 h, 150 °C Hg-rich anneal of $Hg_{0.8}Cd_{0.2}Te$ initially equilibrated at 300 °C in a Te-rich ambient. A is the slope of the interstitial profile in the n-type region (region I). (b) Hg interstitial and vacancy profiles in the junction region after a 2 h, 150 °C, Hg-rich anneal of $Hg_{0.8}Cd_{0.2}Te$ initially equilibrated at 300 °C in a Te-rich ambient. λ is the characteristic length of the decay of interstitials into region II (shown here calculated as the distance it takes to decay $1/e$ from 1.76×10^6 cm^{-3}). Under these processing conditions, λ is 0.036 μm.

This assumption is valid when simulating an anneal in a Hg ambient, ion milling, or junction drive-in following ion implantation.[19]

The interstitial flux in region I is given by

$$J_I = -D_I \frac{\partial C_I}{\partial x} = D_I \left(\frac{C_I^{\text{surface}}}{x_j} \right). \tag{6}$$

The integrated flux of interstitials to the junction, $\int J_I dt$, is equal to the bulk concentration of vacancies, V_{bulk}, times the junction depth,

$$x_j V_{\text{bulk}} = \int_0^t J_I dt. \tag{7}$$

If the concentration of interstitials at the surface reaches a constant value, the drive-in of the junction will be limited by the diffusion of the interstitials through region I to the junction. Integrating Eq. (7) using the flux given in Eq. (6) gives

$$x_j = \sqrt{\frac{2 D_I C_I^{\text{surface}} t}{V_{\text{bulk}}}}. \tag{8}$$

The junction depth is proportional to the concentration and diffusivity of the interstitials and the anneal time. The junc-

tion depth is inversely proportional to the background vacancy concentration, making it difficult to form deep junctions in heavily doped material.

Equation (8) has been used by a number of researchers to calculate the junction depth in HgCdTe as a function of initial and processing conditions.[2–6] It is similar to the parabolic limit of the Deal–Grove model developed to calculate oxide thickness as a function of growth conditions.[15] This model approximates the interface between regions I and II as a sharp step. The concentration of interstitials in region II is assumed to be zero. These assumptions are not valid for the initial, reaction-limited regime and for processing conditions where the junction is broad, such as when there is a low vacancy concentration in the bulk and/or a fast interstitial diffusion coefficient (relative to the recombination rate). Accounting for these conditions requires a more sophisticated model.

IV. DERIVATION OF AN ENHANCED ANALYTICAL MODEL

We now derive a more complete analytical model, which accounts for both the diffusion of interstitials from the surface and the decay of interstitials into region II. The gradient of the Hg interstitial profile in region I is calculated. The interstitial concentration at the junction is not assumed to be zero, allowing determination of the characteristic length and shape of the interstitial decay in region II. The enhanced model gives a closer approximation to the numerical solution and experimental data. Using this model, the junction depth during the initial reaction-limited stage can also be calculated.

In the enhanced model, interstitials and vacancies are still assumed to be in equilibrium in region I so the steady-state, continuity equation, Eq. (4), applies. For a constant source boundary condition, the solution to Eq. (4) is

$$C_I = Ax + C_I^{\text{surface}}, \quad x \leqslant x_j. \tag{9}$$

A, the slope of the interstitials in region I, is shown in Fig. 1(a).

Beyond the junction, the interstitials decay exponentially into region II, as seen in Fig. 1(b). This is due to the finite recombination rate of interstitials and vacancies. The interstitial concentration in this region can be determined from the Hg interstitial continuity equation, Eq. (2), by assuming steady-state conditions and setting the vacancy concentration equal to a uniform background concentration (V_{bulk}),

$$\frac{\partial C_I}{\partial t} = D_I \frac{\partial^2 C_I}{\partial x^2} + g - k_R C_I V_{\text{bulk}} = 0. \tag{10}$$

This expression is valid when the bulk vacancy concentration is much greater than the interstitial concentration. Under these conditions, the equilibration reaction will have a larger effect on the interstitial profile. In low vacancy concentration material or under conditions of high interstitial injection, Eq. (10) is not valid. The solution to Eq. (10) is

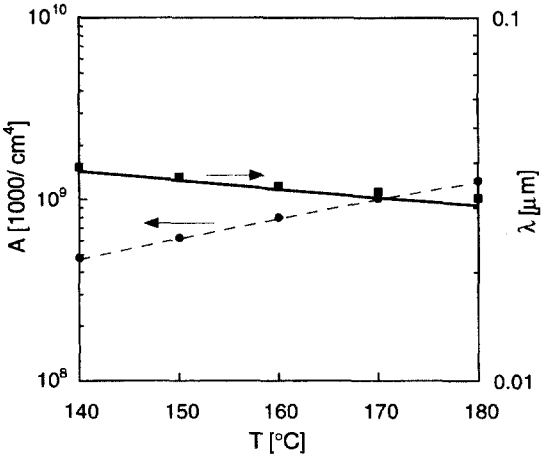

FIG. 2. Analytically and numerically calculated gradients of Hg interstitials in region I, A, and decay lengths of Hg interstitials into region II, λ, for 1 day, Hg-rich anneals at the specified temperatures of $Hg_{0.8}Cd_{0.2}Te$ initially equilibrated at 300 °C in a Te-rich ambient. (The solid line and ■ are λ calculated numerically and analytically, respectively. The dashed line and ● are A calculated numerically and analytically, respectively.)

$$C_I = B \exp\left[-\frac{x}{\lambda}\right] + \frac{g}{k_R V_{\text{bulk}}}, \quad x \geqslant x_j,$$

$$\text{where } \lambda = \sqrt{\frac{D_I}{k_R V_{\text{bulk}}}}. \tag{11}$$

λ is the characteristic length of the exponential decay of Hg interstitials in region II, shown in Fig. 1(b). During the parabolic regime, B is a fictitious surface concentration. However, in the linear, reaction-limited regime, B is the equilibrium interstitial concentration for the Hg-rich boundary condition.

At the junction, the interstitial concentrations and gradients in regions I and II must be equal. A and B are solved for by equating the concentrations calculated in each region [Eqs. (9) and (11)] and their derivatives:

$$A = \frac{\dfrac{g}{k_R V_{\text{bulk}}} - C_I^{\text{surface}}}{x_j + \lambda}, \tag{12}$$

$$B = \lambda \left(\frac{C_I^{\text{surface}} - \dfrac{g}{k_R V_{\text{bulk}}}}{x_j + \lambda} \right) \exp\left[\frac{x_j}{\lambda}\right]. \tag{13}$$

Both A and B are functions of junction depth, and thus, vary with time. λ is time independent. The linear slope, A, and the characteristic tail length, λ, calculated analytically agree with the numerical solutions, as seen in Fig. 2.

With an expression for the slope, A, the flux can be written as

$$J_I = -D_I \frac{\partial C_I}{\partial x} = D_I \left(\frac{C_I^{\text{surface}} - \dfrac{g}{k_R V_{\text{bulk}}}}{x_j + \lambda} \right). \tag{14}$$

In Eq. (6), the flux is a function of only the Hg interstitial diffusion coefficient, the interstitial concentration at the surface, and the junction depth. In the enhanced model, in-

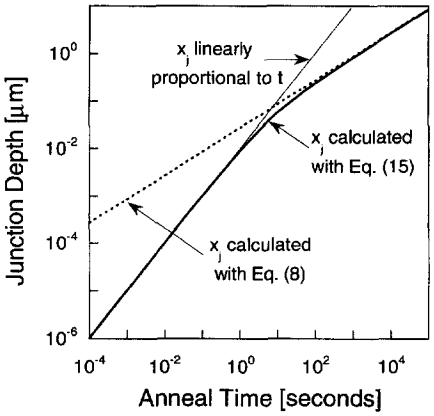

FIG. 3. Junction depths calculated with Eq. (8), the simpler analytical expression, and Eq. (15), the enhanced model, for a 150 °C Hg-rich anneal of $Hg_{0.8}Cd_{0.2}Te$ initially equilibrated at 300 °C in a Te-rich ambient. The enhanced model is needed to resolve the junction depth during the initial, reaction-limited regime.

terstitials in region II are not assumed to be negligible, and the flux is calculated using the difference between the surface and bulk interstitial concentrations. Integrating Eq. (4) using the enhanced equation for the flux, Eq. (14), gives

$$\frac{x_j^2}{2}+\lambda x_j=\frac{D_I}{V_{\text{bulk}}}\left(C_I^{\text{surface}}-\frac{g}{k_R V_{\text{bulk}}}\right)t. \tag{15}$$

This enhanced equation for junction depth differs from Eq. (8) in that it accounts for the width of the junction due to interstitial and vacancy recombination. Figure 3 shows an example of the junction depths calculated with Eqs. (8) and (15). The parameters used are given in Table I.[12,13] Table II lists the equations used to calculate the parameters. Initially, the process is completely reaction limited, and the junction moves linearly with time. The junction drive-in rate decreases once the diffusion rate of the interstitials through region I becomes significant. 500 s into the anneal, the junction depth is proportional to the square root of time, indicating that the process is now completely diffusion limited. During the reaction-limited stage, the enhanced model must be used to accurately calculate the junction depth.

TABLE I. Parameters used in the analytical solution of a 150 °C, Hg-rich anneal. The calculated point defect profiles are plotted in Fig. 4.

Parameter	Value at 150 °C, 2 h
V_{bulk}	5.16×10^{16} cm^{-3}
C_I^{surface}	4.89×10^{9} cm^{-3}
D_I	3.85×10^{-5} cm^2 s^{-1}
g	4.12×10^{10} cm^{-3} s^{-1}
k_R	5.85×10^{-11} cm^3 s^{-1}
λ	3.57×10^{-6} cm
A (2 h)	-2.13×10^{13} cm^{-4}
B (2 h)	2.15×10^{35} cm^{-3}

In the example plotted in Fig. 3, junction depths calculated with Eqs. (8) and (15) converge for longer anneals. This indicates that, under these annealing conditions, the decay of interstitials into region II is very small compared to the junction depth. This places bounds on the interstitial diffusion coefficient relative to the recombination rate. Under certain processing conditions, such as when the bulk vacancy concentration is small and/or the interstitial diffusion coefficient is fast, the two equations will not converge, even at long times. In these cases, Eq. (15) is required to determine junction depth.

A and B can be substituted into Eqs. (9) and (11) to calculate the Hg interstitial profile in regions I and II. The Hg interstitial profile calculated analytically using Eq. (9) in region I and Eq. (11) in region II agrees with that calculated numerically, as seen in Fig. 4. The simulations assume no vacancy diffusion. The parameters used are given in Table

TABLE II. Equations for the parameters used in the numerical and analytical models.

Parameter	Published value (Refs.)	Updated value (Refs.)
C_v^{equil}	$\{2.77\times10^{28}\exp(-1.66\text{ eV/kT})\}/P$ (10)	$\{3.3\times10^{28}\exp(-1.66\text{ eV/kT})\}/P$ (12, 13)
D_v	$1.2\times10^{5}\exp(-1.51\text{ eV/kT})$ (10, 13)	
C_I^{equil}	$1.16\times10^{17}\exp(-.415\text{ eV/kT})\ P$ (10)	$6.09\times10^{15}\exp(-.307\text{ eV/kT})\ P$ (13)
D_I	$2.35\times10^{-3}\exp(-.15\text{ eV/kT})$ (10)	
P(Hg-rich)	$1.32\times10^{5}\exp(-.635\text{ eV/kT})$ (10, 13)	
P(Te-rich)	$4.59\times10^{6}\exp(-1.075\text{ eV/kT})$ (10)	$1.02\times10^{7}\exp(-1.117\text{ eV/kT})$ (13)
g	$1\times10^{40}\exp(-2.3\text{ eV/kT})$ (10)	$1\times10^{38}\exp(-2.3\text{ eV/kT})$ (12, 13)
$k_R=g/C_V^{\text{equil}}C_I^{\text{equil}}$	$g/3.21\times10^{45}\exp(-2.075\text{ eV/kT})$ 10	$g/2.01\times10^{44}\exp(-1.97\text{ eV/kT})$ (13)

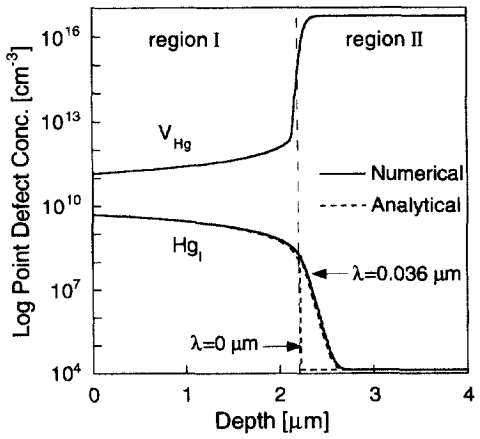

FIG. 4. Hg interstitial profiles calculated analytically from Eqs. (9) and (11) using the parameters in Table II ($\lambda = 0.036\ \mu m$) and using $\lambda = 0$. The numerically calculated Hg interstitial and vacancy profiles are also shown. The simulations are for a 2 h, Hg-rich anneal at a 150 °C anneal of $Hg_{0.8}Cd_{0.2}Te$ initially equilibrated at 300 °C in a Te-rich ambient, assuming negligible vacancy diffusion.

I.[12,13] Figure 4 also plots the Hg interstitial profile calculated analytically by assuming that the junction is sharp (λ is 0). This is the interstitial profile that would be predicted if the decay of interstitials into region II was not accounted for.

The changes in the interstitial concentration over time from the contribution of diffusion, $D_I(\partial^2 C_I/\partial x^2)$, and generation/recombination, $g - k_R C_I C_V$, are seen in Fig. 5. In region I, the contributions from both the diffusion and generation/recombination terms are zero; the interstitial profile does not change with time. The assumptions that the interstitials have reached steady state and are in equilibrium with the vacancies are valid. The vacancy profile can be calculated analytically in region I using the equilibrium expression $C_V = g/(k_R C_I)$. At the junction, the interstitial concentration increases due to diffusion and decreases due to generation/recombination. Equilibrium between the point defects cannot be assumed. In this case, the vacancy concentration in region II must be solved for numerically.

The enhanced model can be used to determine the limits of when the analytical solution fails in predicting the proper junction depth and a numerical model must be used. In order for the analytical model to be accurate, $\lambda \ll x_j$ in the parabolic regime. In other words, the decay of the interstitials into region II must be much smaller than the width of region I. If the decay is long, the interstitials diffuse very fast into the bulk, quickly reaching the backside of the sample. The interstitials build up to their equilibrium value before vacancies can equilibrate with them. Vacancies then decay exponentially with time everywhere in the sample in order to equilibrate with the interstitials. There is no distinct junction, and a numerical model must be used to calculate the broad vacancy profile. From the definition of λ in Eq. (11), it can be seen that a large λ would result from a very high interstitial diffusion coefficient, a low recombination rate, and/or a low background vacancy concentration. When these factors fail to give $\lambda \ll x_j$, the junction depth must be calculated numerically.

The analytical models assume that junction drive-in is dominated by the flux of interstitials to the junction. The flux of vacancies from the bulk to replace those annihilated by injected interstitials is assumed to be negligible. This assumption is invalid when a high anneal temperature is used and/or when the excess Hg interstitial concentration is very small. Bounds are placed on the Hg vacancy diffusion coefficient when the analytical model accurately simulates experimental data. The influence of vacancy diffusion must be negligible in comparison to the drive-in of the junction by the interstitials and their subsequent decay into region II so,

$$\sqrt{D_v t} \ll \lambda \quad \text{and} \quad x_j. \tag{16}$$

Substituting for the definition of λ and rearranging Eq. (16) gives

$$t \ll \frac{D_I}{D_v k_R V_{\text{bulk}}}, \tag{17}$$

which is the time before the vacancy profile begins to smooth out due to vacancy diffusion. It is the limit of time over which the analytical model is valid. For lower tempera-

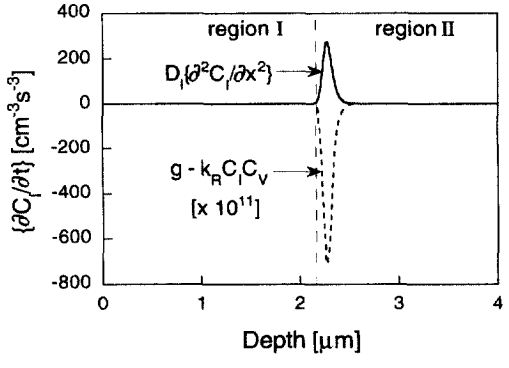

FIG. 5. The change in the interstitial concentration with time due to both diffusion, $D_I(\partial^2 C_I/\partial x^2)$, and generation/recombination, $g - k_R C_I C_V$. At the junction, the interstitial concentration increases due to diffusion and decreases due to recombination with the vacancies. The point defects are not in equilibrium in this region. (This is a numerical simulation of the interstitials for a 2 h, Hg-rich anneal at a 150 °C anneal of $Hg_{0.8}Cd_{0.2}Te$ initially equilibrated at 300 °C in a Te-rich ambient.)

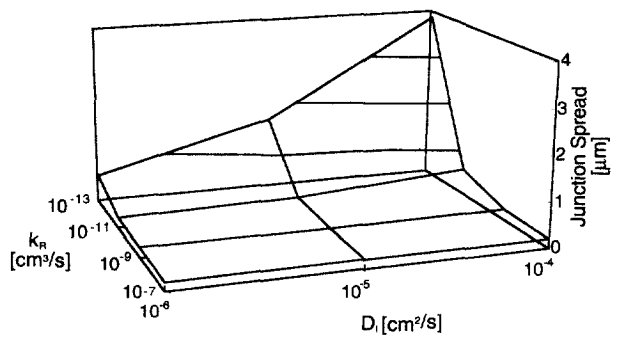

FIG. 6. Junction spread calculated numerically from a 2 h, Hg-rich anneal at 150 °C of $Hg_{0.8}Cd_{0.2}Te$ initially equilibrated at 300 °C in a Te-rich ambient. The junction spread is defined as the distance from 10% to 90% of the bulk vacancy concentration. D_I and k_R were varied while keeping $D_I C_I^{\text{surface}}$ equal to a constant and g/k_R equal to $C_I^{\text{equil}} C_V^{\text{equil}}$. The junction broadens with increasing D_I and decreasing k_R due to the increased distance that interstitials diffuse into region II before recombining with vacancies.

tures, where D_V is negligible, the analytical model is valid for long times.[3,5,6] The analytical model fails in a very short time at higher temperatures due to fast vacancy diffusion.[5]

In order to accurately resolve the point defect concentrations at the junction, the grid spacing in a numerical simulation must be small enough to resolve the changes taking place in the junction region. Therefore, the analytically calculated λ places an upper bound on the grid spacing used in a numerical simulation. Under conditions where λ is large (high temperatures and/or lightly doped vacancy material), the grid spacing may be limited by other factors.

The accuracy of the junction depth calculated by either analytical or numerical methods depends upon the accuracy of the parameters used in the model, especially D_I, C_I^{surface}, k_R, and V_{bulk}. The vacancy concentration has been measured as a function of annealing temperature and Hg pressure.[20,21] The $D_I C_I^{\text{surface}}$ product has been determined from Hg self-diffusion experiments, but the individual parameters cannot be resolved independently.[12,13] The sensitivity of junction spread (calculated numerically) to D_I and k_R (keeping $D_I C_I^{\text{surface}}$ equal to a constant and g/k_R equal to $C_I^{\text{equil}} C_V^{\text{equil}}$) is shown in Fig. 6. Increasing D_I or decreasing k_R causes λ to increase, Eq. (11). This is because interstitials diffuse further into region II before recombining with vacancies. Therefore, variations in D_I and k_R used in the model result in variations in the calculated junction spread and junction depth.

V. SUMMARY

N-on-p junction formation in HgCdTe can be described analytically by modeling the concentration of interstitials in the n-type region with a linear gradient and the junction region as a sharp step. The model is based on the parabolic limit of the Deal–Grove model for oxide growth on silicon. The junction depth estimated by this equation is not accurate in the linear, reaction-limited regime or during processing conditions where the junction width is significant.

An enhanced analytical model has been developed in which Hg interstitials are not assumed to be negligible at the junction. The interstitial concentration decays exponentially into the p-type region due to a finite recombination rate between interstitials and vacancies. The model can be used to calculate the slope of the interstitial concentration in the n-type region. The characteristic length of the exponential decay of interstitials into the p-type region is also determined.

The junction depth predicted by the more detailed analytical model differs from the simplified model in that it accounts for the decay of interstitials into the p-type region. This model is necessary to determine junction depth during the initial, reaction-limited regime of junction formation. The junction depth, under processing conditions where the width of the junction is significant relative to the junction depth, can also be calculated. The enhanced analytical model can be used to determine the limits of when the junction depth estimated analytically is valid. The decay length of interstitials also places an upper bound on the grid spacing used in numerical simulations.

Junction formation in extrinsically doped HgCdTe can be modeled using similar analytical techniques. The junction depth will depend on both the background dopant concentration and the vacancy concentration. The rate of kick-out between dopant atoms and Hg interstitials will affect the characteristic length of the Hg interstitial tail. The analytic technique detailed in this paper can also be used to simplify a wide array of problems in other materials systems, such as transient enhanced diffusion in Si. While numerical models of junction formation give accurate solutions for the point defect profiles, analytical techniques provide enhanced insight into the junction formation process and offer a quick means of estimating junction depths.

ACKNOWLEDGMENT

The authors would like to thank B. L. Williams at Stanford University for helpful discussions and for providing experimental data for calibrating the models.

[1] M. A. Berding, M. van Schilfgaarde, and A. Sher, Phys. Rev. B **50**, 1519 (1994).
[2] E. Belas, P. Hoschl, R. Grill, J. Franc, P. Moravec, K. Lischka, H. Sitter, and A. Toth, Semicond. Sci. Technol. **8**, 1695 (1993).
[3] D. T. Dutton, E. O'Keefe, P. Capper, C. L. Jones, and S. Mugford, Semicond. Sci. Technol. **8**, S266 (1993).
[4] V. V. Bogoboyashchii, A. I. Elizarov, V. I. Ivanov-Omskii, V. R. Petrenko, and V. A. Petryakov, Sov. Phys. Semicond. **19**, 505 (1985).
[5] C. L. Jones, M. J. T. Quelch, P. Capper, and J. J. Gosney, J. Appl. Phys. **53**, 9080 (1982).
[6] H. F. Schaake, J. H. Tregilgas, J. D. Beck, M. A. Kinch, and B. E. Gnade, J. Vac. Sci. Technol. A **3**, 143 (1985).
[7] L. O. Bubulac, W. E. Tennant, D. S. Lo, D. D. Edwall, J. C. Robinson, J. S. Chen, and G. Bostrup, J. Vac. Sci. Technol. A **5**, 3166 (1987).
[8] L. O. Bubulac and W. E. Tennant, Appl. Phys. Lett. **51**, 355 (1987).
[9] B. L. Williams, H. G. Robinson, and C. R. Helms, Appl. Phys. Lett. **5**, 692 (1997).
[10] J. L. Melendez and C. R. Helms, J. Electron. Mater. **24**, 565 (1995).
[11] J. L. Melendez and C. R. Helms, J. Electron. Mater. **24**, 578 (1995).
[12] C. R. Helms, J. L. Melendez, H. G. Robinson, S. Holander, J. Hasan, and S. Halepete, J. Electron. Mater. **24**, 1137 (1995).
[13] S. Holander, H. G. Robinson, and C. R. Helms, Mater. Res. Soc. Symp. Proc. **389**, 47 (1995).
[14] J. L. Melendez and C. R. Helms, J. Electron. Mater. **22**, 999 (1993).
[15] B. E. Deal and A. S. Grove, J. Appl. Phys. **36**, 3770 (1965).
[16] M. E. Law, Ph.D. thesis, Dept. of Electrical Engineering, Stanford University (1988).
[17] D. Mathiot and J. C. Pfister, J. Appl. Phys. **66**, 970 (1989).
[18] H. G. Robinson, M. D. Deal, G. Amarantunga, P. B. Griffin, D. A. Stevenson, and J. D. Plummer, J. Appl. Phys. **71**, 2615 (1992).
[19] S. Holander-Gleixner, H. G. Robinson, B. L. Williams, and C. R. Helms, J. Electron. Mater. **26**, 628 (1997).
[20] H. R. Vydyanath, J. Electrochem. Soc. **128**, 2609 (1981).
[21] H. F. Schaake, J. Electron. Mater. **14**, 513 (1985).